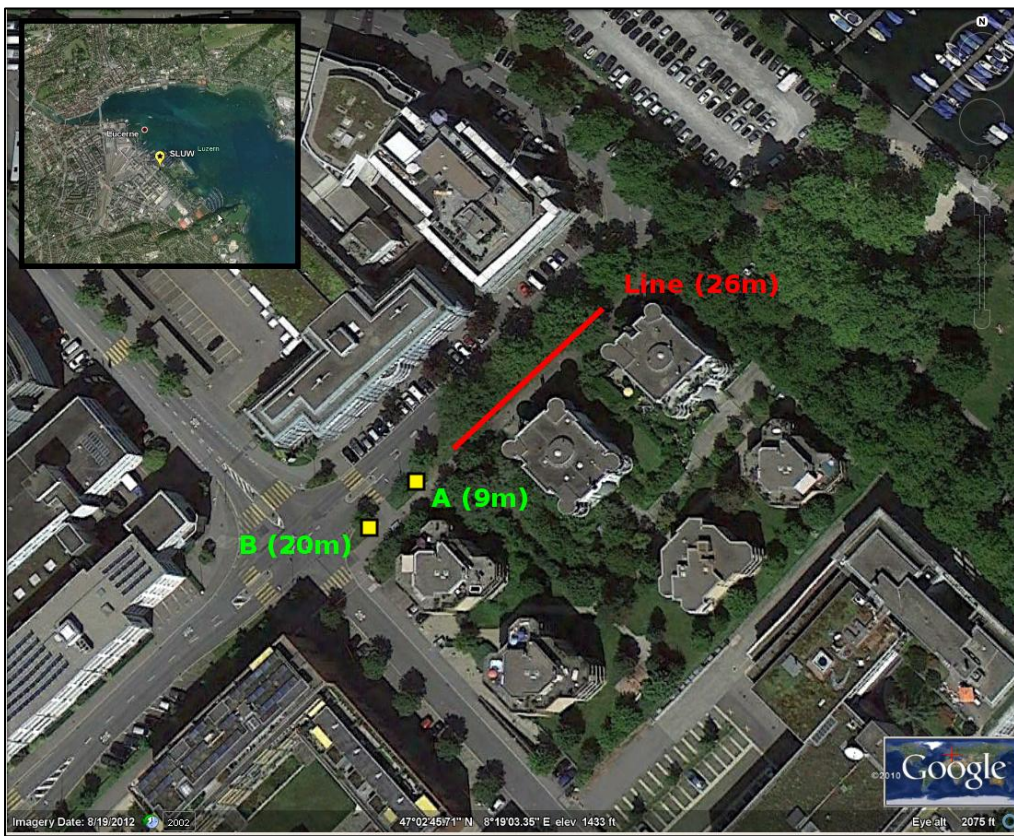# Station SLUW
Report on active seismic experiment

Introduction

In date 14.04.2011 an active seismic experiment has been performed in Luzern at the location of the strong motion station SLUW (Figure 1), with the aim of mapping the phase velocity dispersion function of the surface-waves at high-frequency (>10Hz). The goal of the experiment is to extend the resolution of a previous passive seismic survey on the shallower part of the velocity model. For the measurement, two types of instrumentation were used together (Figure 2); an array of 24 vertical geophones (10Hz corner frequency, GEODE system), with 1m distance between, and an array of 6 two-channel seismological stations, with 2m inter-distance. Combining these two equipments theoretically allows having the large spatial resolution (from the dense geophone array) together with the possibility of using three component recordings.

Figure 1. *Location of the seismic line (in red) and the two wave-filed excitations (A at 9m and B at ~20m) with yellow squares.*

Each seismological station was equipped with two three-component velocity seismometers (Lennarz 3C, 5s eigenperiod) and a 24bit data-logger (Quanterra Q330). Synchronization between stations was assured by standard GPS, while a more accurate differential GPS (Laica Viva system) was used to precisely locate the sensor coordinates with a tolerance of less than 5cm.

Figure 2. *The surface-wave survey line. In the picture, only the 12 high-resolution three-component seismological stations are visible, while the geophone string of 24 elements is hidden in the grass.*

The acquisition phase

For the experiment, a special device was use as active source, consisting of mass of 120Kg, dropping from a high of 1 and 2m (see Figure 3). Two shot-offset distances were tested (9 and 20m) because the distance at which the surface-waves start developing from the source is generally unknown (without some prior knowledge on the local velocity structure). Ten consecutive wave-field excitations have been performed for each source off-set, with the goal of improving the signal-to-noise ratio by stacking in the time (classical f-k method, CIT.) or in the frequency (wavelet t-f-k method, Poggi et al. 2012) domain.

For the each wave-filed excitation, a recording of about 2s was performed when using the GEODE data-logger. These consecutive recordings have been then merged in a

unique continuous stream of data, removing the noisy tail of the traces (Figure 4). Conversely, the seismological stations recorded continuously, so that a manual selection of the usable part of the recoding had to be performed. It has to be noticed that not all the shots were identically successful during the experiment. Therefore, a further selection on the quality of the performed wave-field excitation has been performed. As such, only the best shots were selected and gathered into a continuous stream.


Figure 3. *The 120kg dropping mass device which has been used as artificial source to stimulate the generation of Rayleigh waves.*

Processing
From the geophone recordings only the vertical direction is available for processing, while from the seismological stations both the vertical (channel 3) and the radial (channel 2, "North") directions of recording have been analyzed (Figure 5 and 6). In all cases the classical f-k approach and the t-f-k analysis (Poggi et al., 2012) have been used, providing nevertheless comparable results. In this report, then, only the results from the second method are presented, which generally provides a less noisy representation of the higher modes. A tentative analysis of the transversal direction was also made, but the results have not been included in this report, since the employed source does not give the possibility to directly generate anti-plane motion, and it is consequently not possible to rely on those results (Figure 6 B). Therefore, the following

considerations are representative of Rayleigh-wave dispersion only. By comparing the two shot offsets, better results were obtained using the lager distance (20m), especially for the generation of the higher modes.

A)

B)
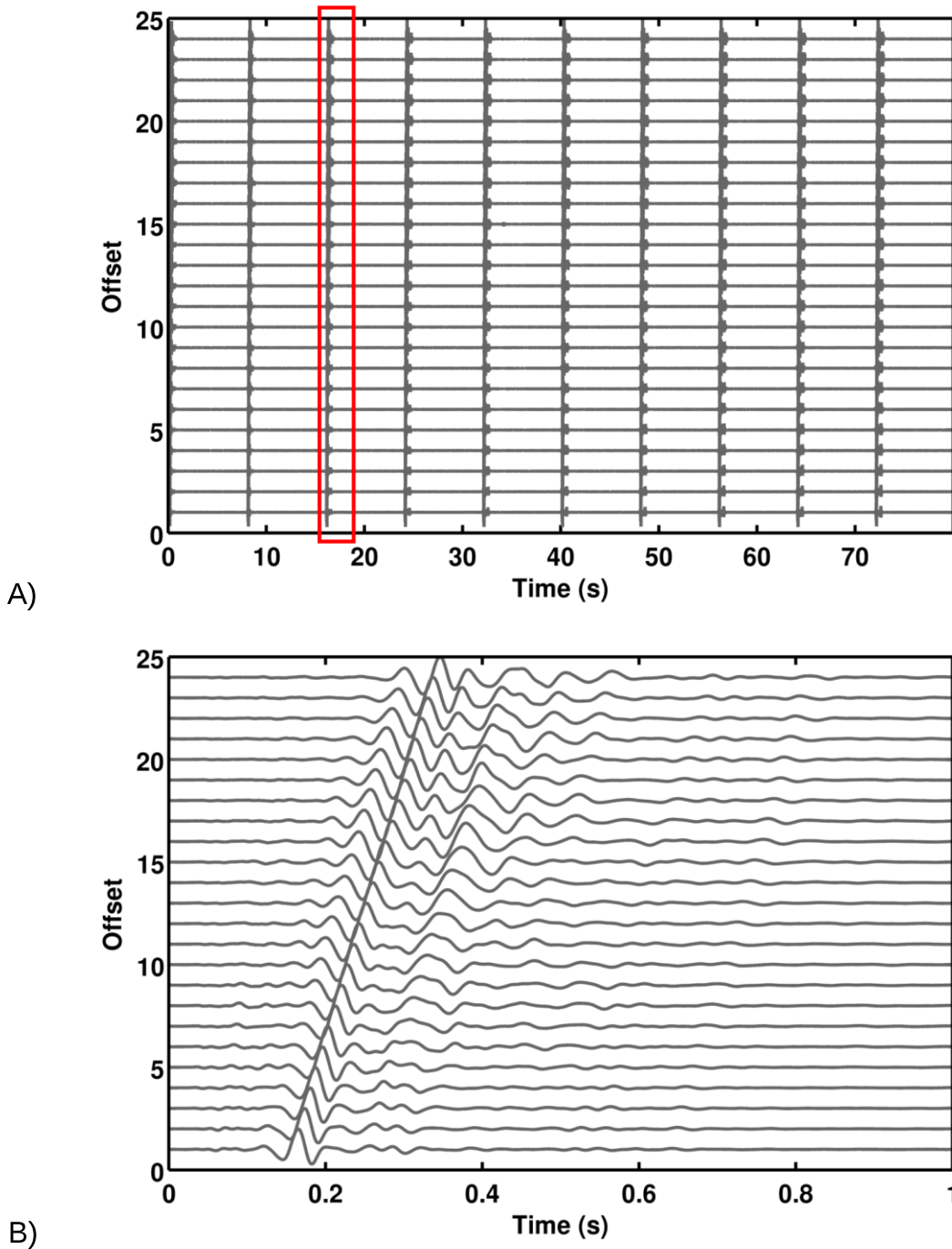
Figure 4. *In A, an example of ten consecutive wave-field excitations using the 120kg dropping mass recorded from the geophone line. In B, detail of the one single shot of the same line (marked in red).*

The results from using the two equipments are mostly comparable (figure 5). Several surface wave modes are clearly identifiable in the velocity-frequency plane. The fundamental mode is stable at the velocity of about 120m/s, up to 15Hz; here a jump in the mode is present, which is however difficult to interpret at this stage; it can be either attributed to an external disturbance in the processing or to a feature of the modes (mode osculation and jump). Two different interpretations has been then proposed (Figure 7). In the first, we propose an exchange of energy between the fundamental mode and the first higher at the osculation point. According to such interpretation, the fundamental mode is no more visible above 15Hz, as all the energy transfers to the above mode. In the second interpretation, on the contrary, the mode is considered unique till 40Hz, with just a weak velocity inversion. Unfortunately, we don't have any mean to propend for an interpretation or for the other at the present level of knowledge. Assessing the reliability of the two hypotheses can be nevertheless done a-posteriori, after analyzing the results of the inversion phase. On the other side, interpretation of the results from the processing of the radial component provided consistent results with the vertical, so that a unique model was finally provided.

A priori information
To reduce the non-uniqueness of surface wave dispersion curve inversion, prior information was added to the velocity model. In particular, the variability in the shallower part of the velocity profile has been limited by including the results from a CPT test, together with a rough S-wave travel-time analysis of the progressing CPT probe (figure 8 and figure 9). This was useful in particular to verify the presence of a possible velocity inversion in the first meters (< 5m). Conversely, the variability in the lowermost part of the velocity profile was constrained by the information from a previous large array survey performed in a nearby site (SBB train station, Poggi et al 2011).

Inversion
For the inversion, a six-layer model was used. Search parameters were basically the layer thickness and the seismic velocities (P and S). These last were allowed to vary according to a range of Poisson's ratio between 0.1 and 0.4. Density was imposed to be constant (due to its little sensitivity to the phase velocity dispersion) at a value of about 2200Kg/m3 for the soft sediment part and 2800 for the bedrock. As already stressed, parameter search bounds were constrained using a-priori knowledge from a CPT and an ambient vibration survey performed in a nearby site (Poggi et al., 2011).

Various inversion attempts were performed, using the different modal interpretations and data selections. As first the two interpretations from the active seismic survey were tested. The first interpretation (Figure 7) required for a reasonable data fit the presence of a too strong velocity inversion in the uppermost layer. Please note that, although the use of velocity inversions improved the fitting of the data, this approach has to be used carefully, as it might lead to unstable and/or unrealistic solutions. Such model, moreover, is not supported by observation from CPT analysis, and therefore this interpretation was rejected from any subsequent analysis. The second interpretation, conversely, provided consistent results. In this case, however, the inverted velocity model was capable to fully explain the fundamental and the first higher mode only.

A)
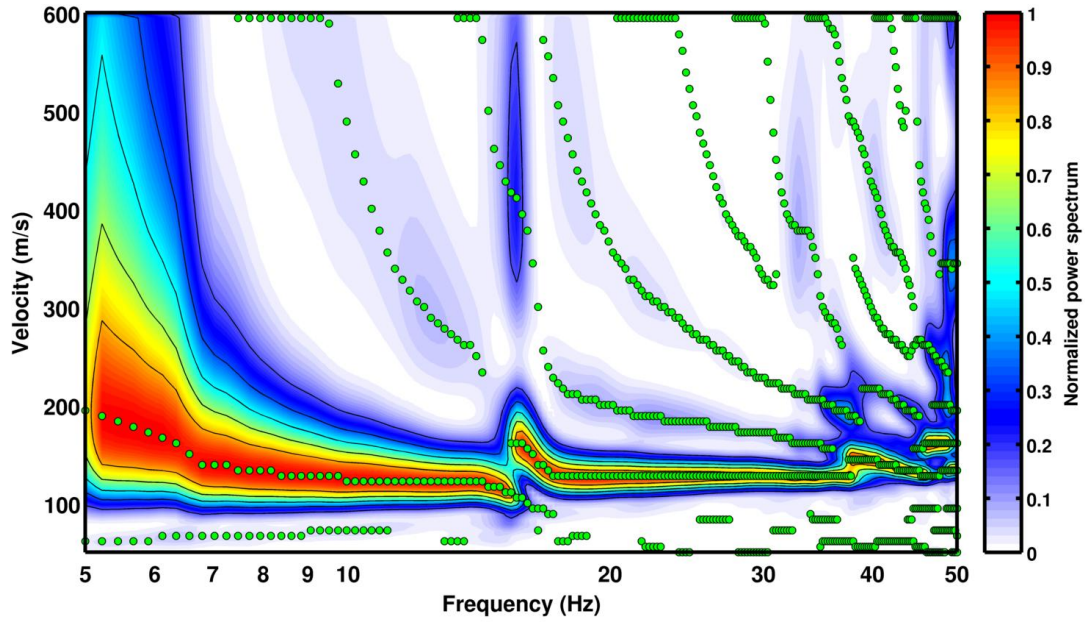
B)
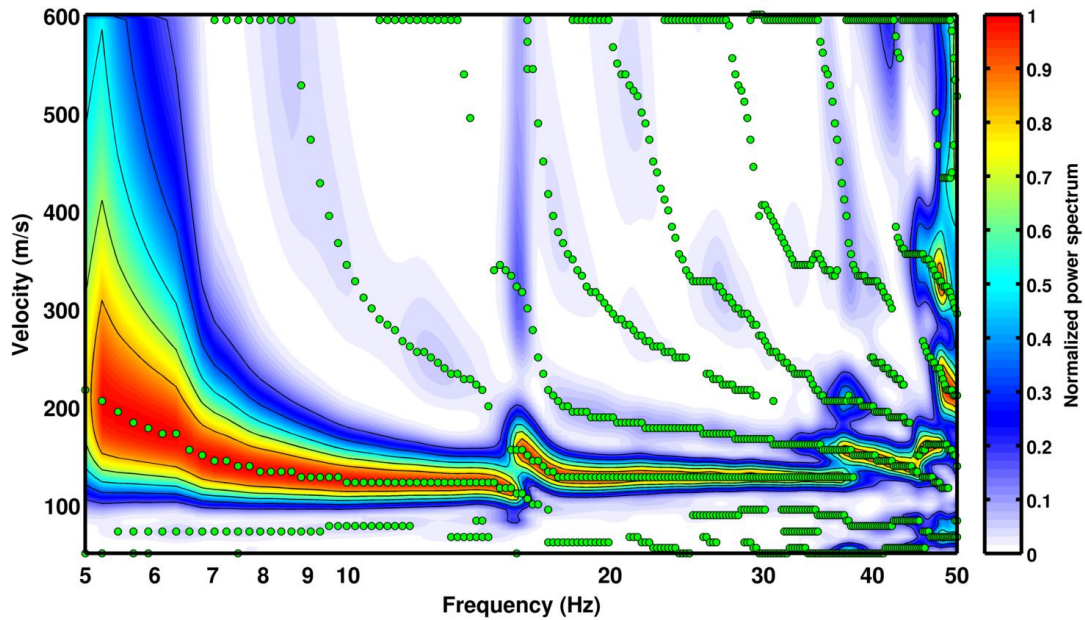
Figure 5. *Results of processing the vertical direction using the geophone string (A) and the Lennartz sensors (B). In both cases, the analysis was performed with the wavelet t-f-k approach. Due to the different number of sensor employed (and therefore resolution) a progressive mismatching is visible for the high-modes. To be conservative, only the fundamental and the first higher mode have been considered for the inversion.*
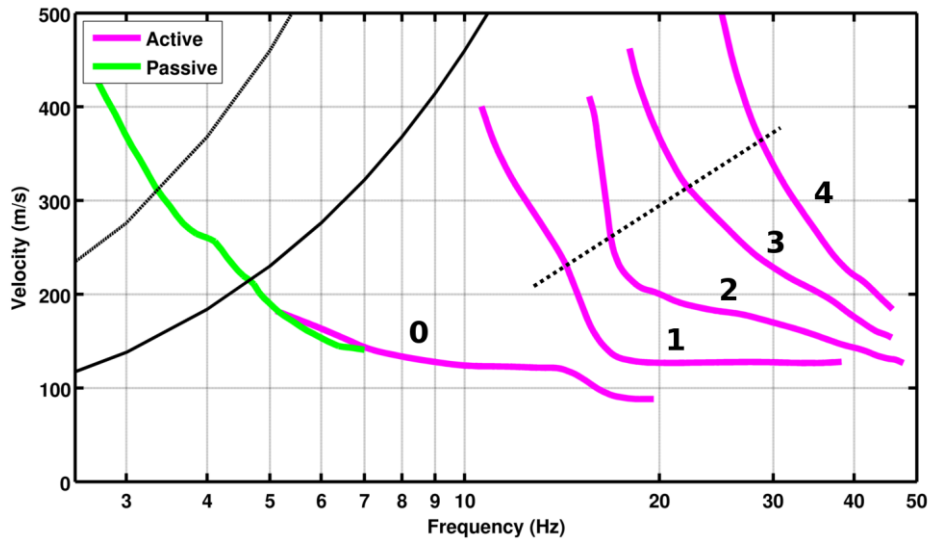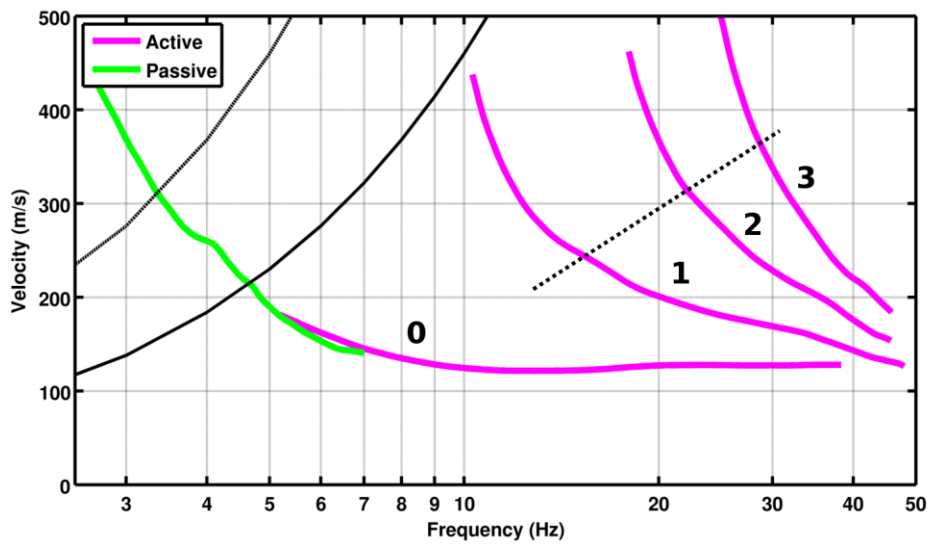
A)
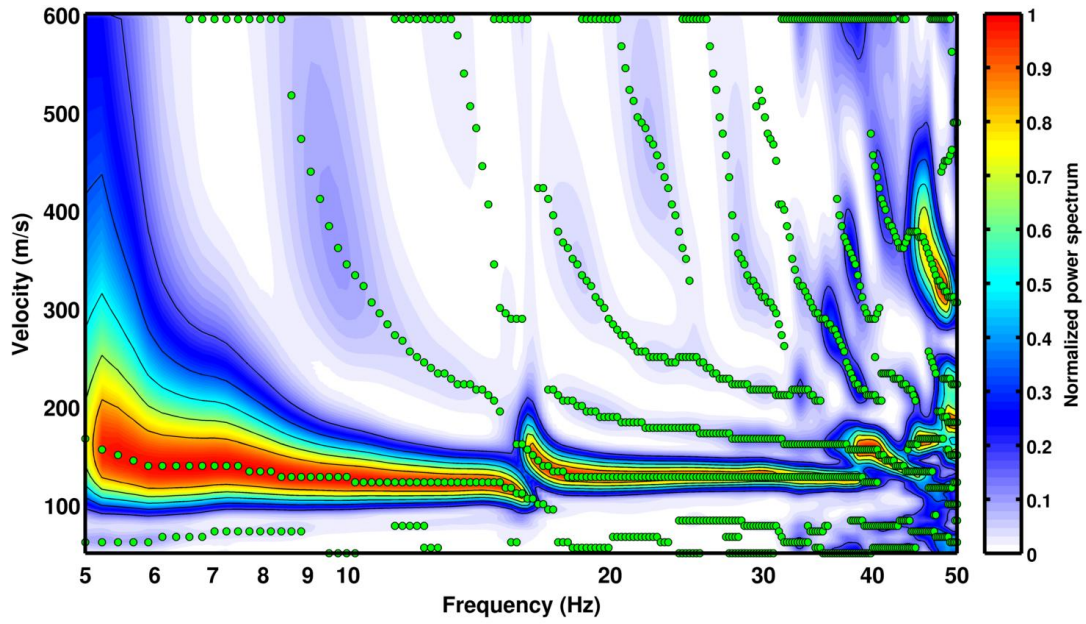
B)
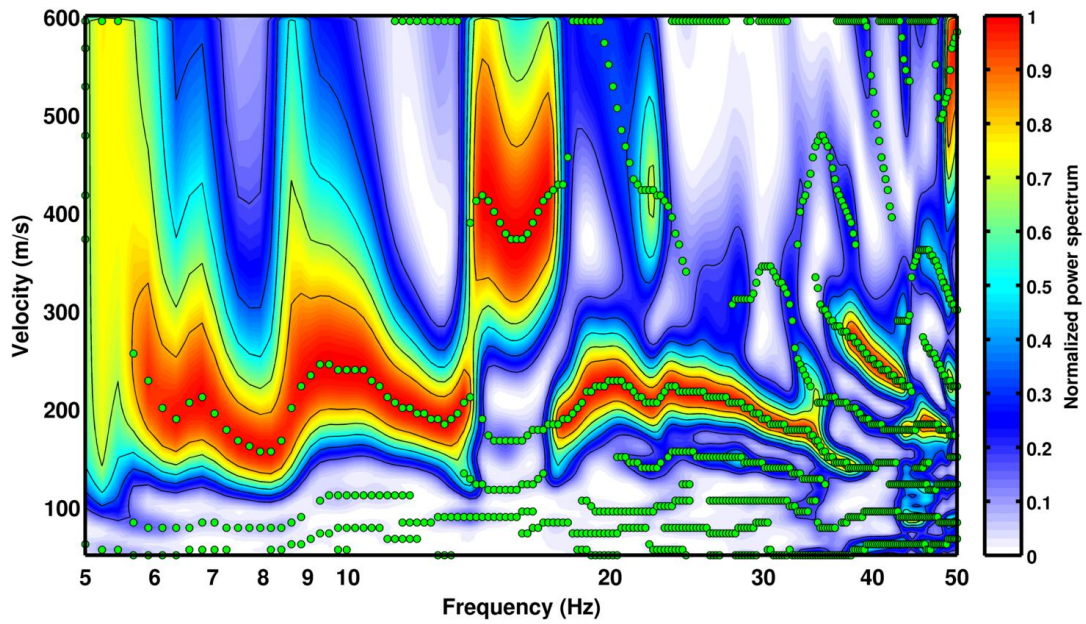
Figure 6. *Results of processing the radial direction (A) and the transversal (B) using the Lennartz sensor array. This last is not realistic and is therefore not used for the inversion, as the employed source cannot excite motion in this direction.*

Figure 7. *Comparison between the two interpretations of the modal dispersion pattern form the f-k spectrum in figure 5B. The fundamental mode is in good agreement with the result from a passive array survey performed on the same area The black dashed line indicates the limits over which the higher modes are not considered any more reliable.*

Modes higher than the first one are probably too uncertain to be included in the analysis, as it can be deduced from the energy level in the f-k spectrum. Also the comparison between the Geode and Quanterra results shows a not always perfect matching of the second and the third higher mode. For this reason, these modes were then not included in the final inversion model.

To better resolve the deeper portion of the velocity model, the fundamental mode of the Rayleigh velocity dispersion curve have been extended at low frequency by adding the results from a passive acquisition survey (vertical component). This gave the possibility to extend the curve from 6Hz down to about 2.5Hz (Figure 7). Complementary, to constraint on the bedrock interface below the sedimentary cover, which is ideally not resolved directly by the dispersion information, the Rayleigh wave ellipticity function has been analyzed by including the horizontal-to-vertical spectral ratio from single station recording of ambient vibration. The H/V curve was computed using the time-frequency wavelet approach proposed by Kristekova (Fäh at al., 2009). At first, only a small portion of the Rayleigh ellipticity curve (the right flank, Fäh at al., 2003) was used, together the value of the site fundamental frequency (f^0=~1.1Hz). After some trials, it was possible to obtain a reliable data fit also for the left flank of the curve, adding useful information on the velocity contrast between sediment fill and bedrock.
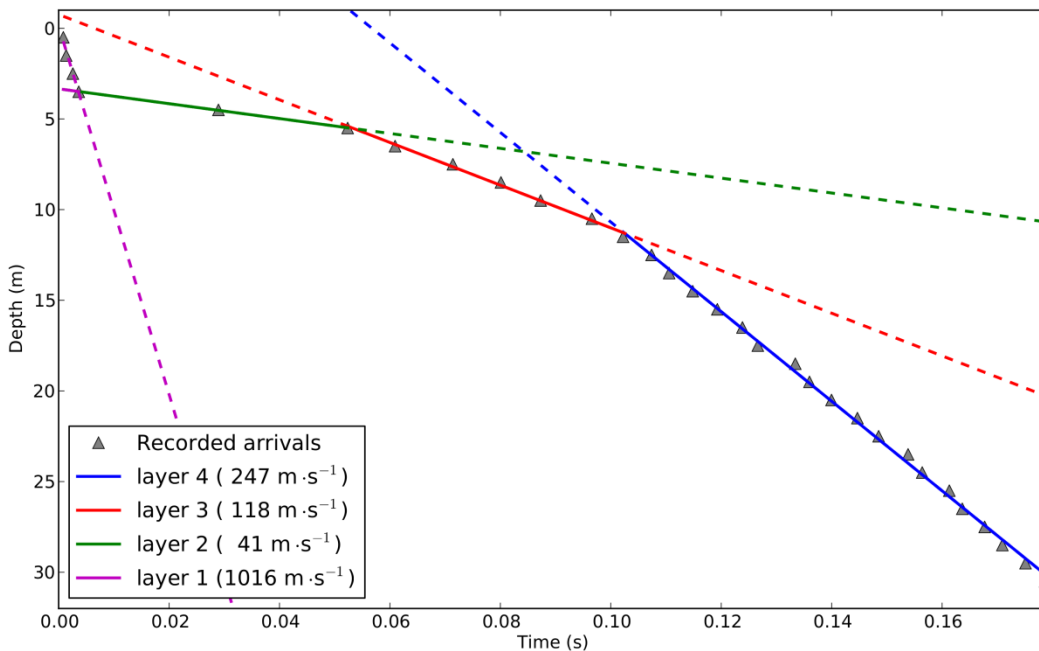

Figure 8. *Travel time analysis from the seismic monitoring of the CPT testing. The picked signals are generated from the progressing of the probe into the ground and recorded at the surface. From the analysis of these hodochrones, at least four layers are interpretable; the second layer, however, might be questionable and should be better integrated into the third one.*
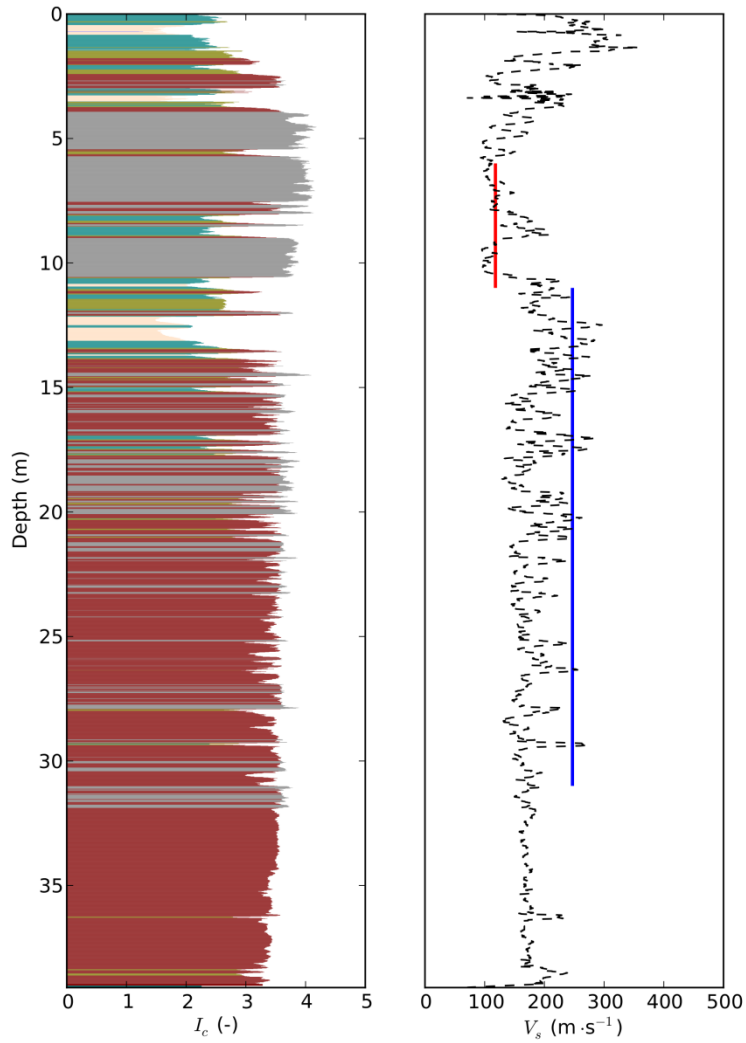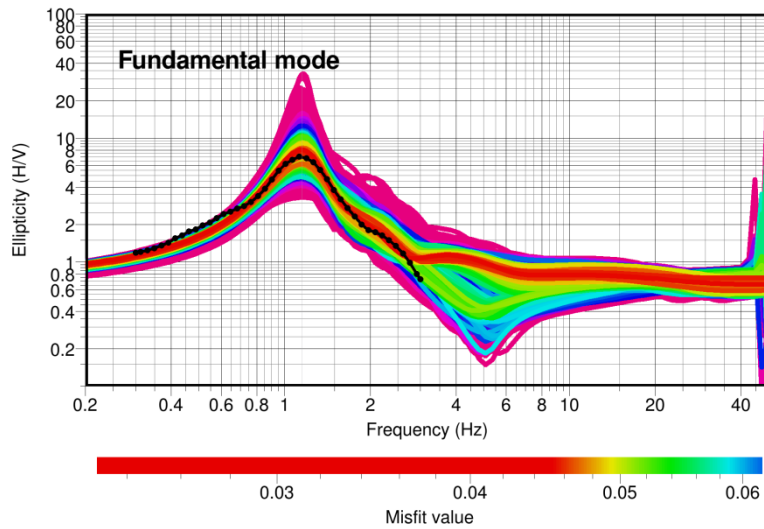
Figure 9. *Comparison of the results from CPT (on the left) and the related travel-time analysis (on the right) for the uppermost 40m of the soil profile of the station SLUW. A small velocity inversion is visible within the first 10m, which was then used as a priory for the following optimization procedure.*
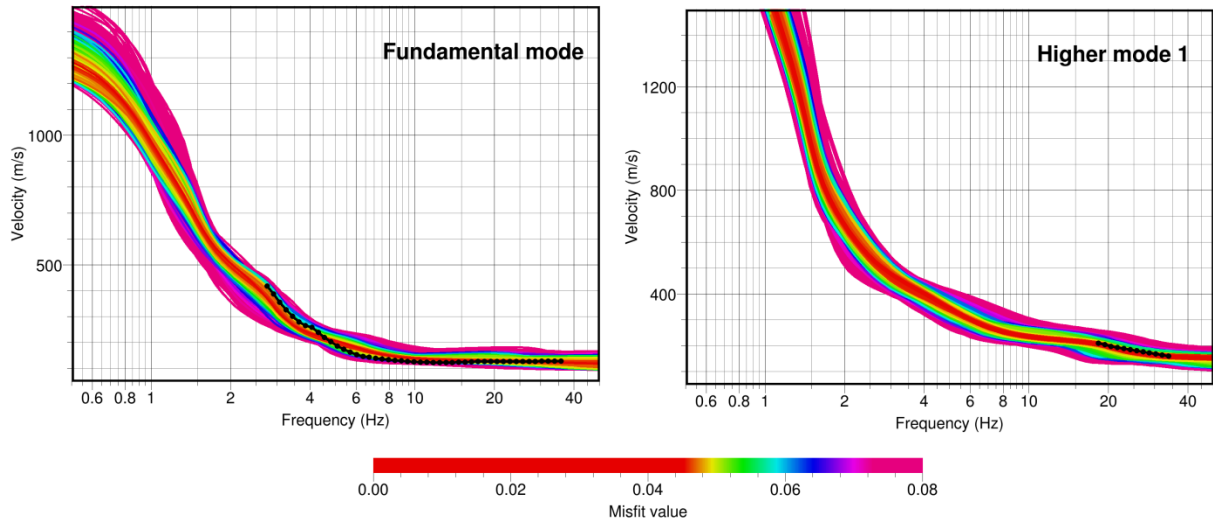
Figure 10. *A) Fit of all the dispersion curves generated during the inversion procedure, and sorted by increasing misfit. A reasonable fit is obtained for both the Rayleigh wave fundamental and first higher mode. B) Fitting of the ellipticity function from single station time-frequency analysis of ambient vibrations. In this case both flanks show a reasonable match, as well as the resonance peak.*

Interpretation

The final velocity model (figure 11) consists in a low-velocity part with a small velocity inversion in the first 10 meters (figure 12B), followed by a progressive increase below this depth, from about 300 to 1000m/s. The larger velocity contrast is found at about 200m (the bedrock interface), which is probably constrained by the use of the ellipticity information in the optimization. The bedrock velocity appears to be realistic (around 1800m/s), but should be confirmed from independent analysis. Overall the velocity model is consistent with a previous preliminary microzonation study of Lucerne (Poggi et al. 2011), where a simplified modes consisting in a 10m low-velocity layer followed by a gradient was proposed.
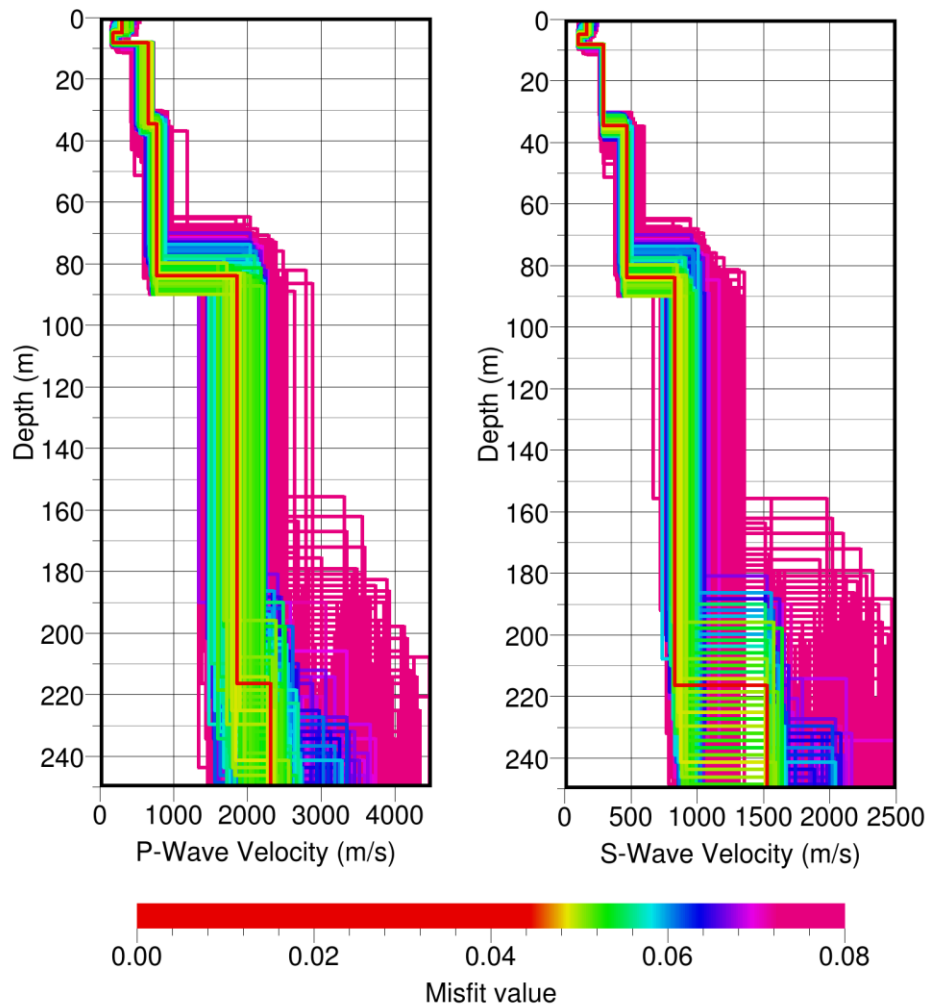
Figure 11. *Ensemble of all the velocity profile modes (Vp on the left and Vs on the right) generated during the inversion (here the data from run 7) and sorted by increasing data misfit. Color-scale is compatible with that of figure 10.*
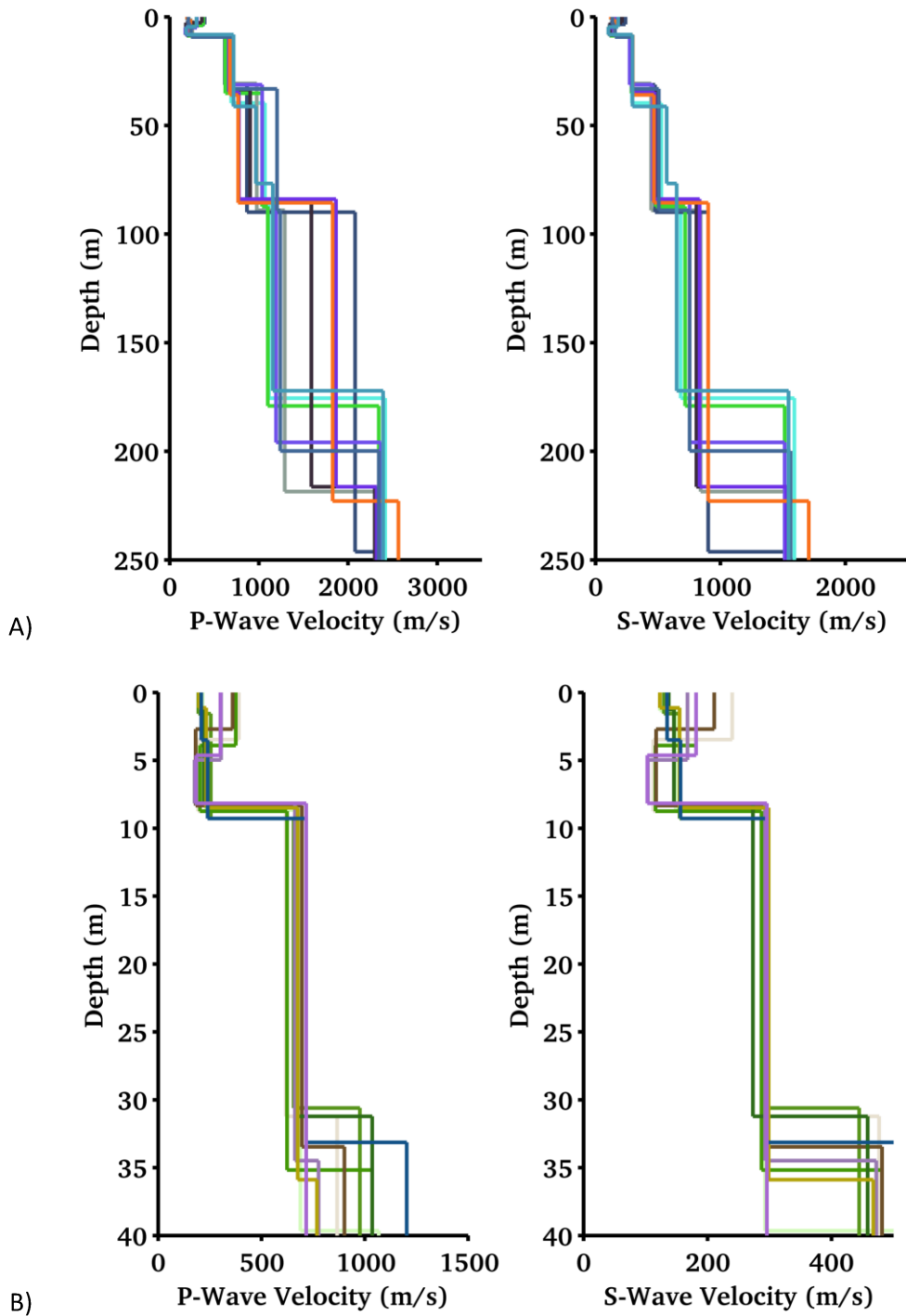
Figure 12. A) *Comparing the best fitting models of 10 different inversion runs (obtained using different initial seeds). These profiles are probably constrained down to 60~80m from the available dispersion curves (from active and passive). The bedrock at about 200m is complementary controlled by the ellipticity information. B) Zoom of the first 40m of the models in A.*

References

Fäh, D., Kind, F. & Giardini, D., 2003. Inversion of local S-wave velocity structures from average H/V ratios, and their use for the estimation of site-effects. J. Seismol., 7, 449–467.

Fäh, D. et al., 2009. Using ellipticity information for site characterisation, NERIES JRA4 "Geotechnical Site Characterization", taskB2-D4, final report.

Poggi, V., Fäh, D. and D. Giardini, 2012. T-f-k analysis of surface waves using the continuous wavelet transform, Pure and Applied Geophysics, Volume 170, Issue 3 , 319-335

Poggi, V., Fäh, D., Burjanek, J. and Giardini, D., 2011. The use of Rayleigh wave ellipticity for site-specific hazard assessment and microzonation. An application to the city of Luzern (Switzerland). Geophys. J. Int., Volume 188, Issue 3, 1154-1172